Journal of Food Engineering 156 (2015) 31–38

Contents lists available at ScienceDirect

Journal of Food Engineering

journal homepage: www.elsevier.com/locate/jfoodeng

Influence of freezing temperature and maltodextrin concentration on stability of linseed oil-in-water multilayer emulsions

Silvana A. Fioramonti [a], Carolina Arzeni [b], Ana M.R. Pilosof [b], Amelia C. Rubiolo [a], Liliana G. Santiago [a,*]

[a] Grupo de Biocoloides, Instituto de Tecnología de Alimentos, Facultad de Ingeniería Química, Universidad Nacional del Litoral, Santa Fe, Argentina
[b] Departamento de Industrias, Facultad de Ciencias Exactas y Naturales, Universidad de Buenos Aires, Buenos Aires, Argentina

ARTICLE INFO

Article history:
Received 26 September 2014
Received in revised form 12 January 2015
Accepted 18 January 2015
Available online 31 January 2015

Keywords:
Multilayer emulsion
Layer by layer deposition
Linseed oil
Whey protein
Alginate
Maltodextrin

ABSTRACT

The effect of maltodextrin (MDX) concentration on the stability of multilayer linseed oil-in-water emulsions before and after freeze–thawing has been studied. Interfacial double-layer emulsions were obtained by performing electrostatic deposition of sodium alginate (SA) onto whey protein isolate (WPI) coated oil droplets at pH 5 (10 wt% oil, 1 wt% WPI 0.25 wt% SA). MDX was also added to emulsions formulation in different concentrations (0–20 wt%), and the systems were then stored at two freezing temperatures (−18 and −80 °C). Stability of emulsions was studied using droplet size, ζ-potential, as well as microstructure determinations and monitoring backscattering profiles versus time. Non-frozen emulsions showed smaller droplet sizes at higher MDX concentrations thus reducing creaming mechanisms and improving emulsion stability. In the absence of MDX, emulsions were highly unstable after freeze–thawing and destabilized faster at −18 °C than at −80 °C, which was attributed to the formation of larger ice crystals at slower freezing rates that promoted interfacial membrane disruption leading to extensive droplet coalescence and oiling off. Both systems showed macroscopic phase separation within the first hour of analysis. The addition of MDX greatly improved emulsion stability after freezing, as emulsions showed no phase separation after thawing during one week storage. This behavior was attributed to MDX cryoprotectant effect, that could have considerably reduce the amount of ice formed during freezing, thereby maintaining the integrity of the interfacial WPI–SA bilayer surrounding oil droplets. Our results suggest that 20 wt% MDX emulsions were the most stable systems both to creaming destabilization and to freeze–thawing processes.

1. Introduction

Oil-in-water emulsions are widely used by the food industry not only in the formulation of conventional products such as sauces, soups, desserts, fruit beverages, ice cream and soft drinks, but also for the development of engineered functional foods that could provide consumers health benefits beyond basic nutrition by the incorporation of bioactive compounds (McClements, 1999; Rodea-González et al., 2012; Carneiro et al., 2013). However, there are many environmental stresses during processing operations (chilling, shearing, dehydration, cooling) that may adversely affect the stability of emulsions, which is strongly influenced by the nature of the interfacial membrane surrounding the oil droplets (Guzey and McClements, 2006). Freezing storage is often used in the food industry either to maintain microbiological and chemical stability or simply as a necessary part of the final product. Nevertheless, many emulsions become physically unstable when frozen, and rapidly breakdown after thawing, through flocculation, coalescence and creaming mechanisms (Palazolo et al., 2011; Ghosh and Coupland, 2008). It is therefore necessary for food technologists to systematically design the physicochemical properties of the interfacial film surrounding the oil droplets by controlling its composition, thickness, electrical charge (Wu et al., 2012; Thanasukarn et al., 2006), so as to create emulsion-based products that have better resistance to freezing conditions and long-term shelf-life. There is a novel technology which relies on the formation of multilayers around emulsion droplets using a layer-by-layer electrostatic deposition technique. Multilayer emulsions consist of oil droplets dispersed in an aqueous medium, coated by an interfacial membrane formed by self-assembly of oppositely charged polymers via electrostatic interactions (McClements et al., 2007). These systems represent a suitable strategy for the encapsulation of sensitive nutraceuticals, particularly those containing omega-3 polyunsaturated fatty acids (PUFAs), since it has been demonstrated that dietary intake of these bioactive components, could provide

* Corresponding author. Tel.: +54 342 4571252x2602.
E-mail address: lsanti@fiq.unl.edu.ar (L.G. Santiago).

http://dx.doi.org/10.1016/j.jfoodeng.2015.01.013
0260-8774/

active protection against coronary heart disease and play an important role in early child nutrition (Innis, 2007; Rodea-González et al., 2012). Indeed, as PUFAs are susceptible to oxidative deterioration, microencapsulation appeared to be a feasible technology to protect them against strong oxidants such as light, heat and oxygen. In previous work, we have established the best conditions required for producing stable multilayer emulsions as encapsulation matrices for the delivery of linseed oil – a vegetable oil with high ω-3 PUFAs content – where lipid droplets were coated by an outer polysaccharide layer (alginate) electrostatically adsorbed to an inner protein layer (whey protein isolate) (Fioramonti et al., 2015). The next step would require dehydration of these emulsions so as to obtain a powdered additive – that could be further incorporated into a food matrix – thereby promoting easier handling and reducing both transportation costs and storage space. Freeze–drying processes, which comprise the removal of water by sublimation from the frozen state (ice), are often used for dehydrating food products when heat-sensitive compounds need to be protected. Nevertheless, this method requires a freezing step prior to dehydration. Thus, for many applications, it is therefore important that emulsions not only exhibit high resistance to freezing processes but also maintain their initial properties when thawed.

Given that sugars are natural occurring cryoprotectants in freeze-tolerant plants and animals (Ghosh et al., 2006), it was expected that they might exert a similar role in frozen food emulsions. Maltodextrins (MDX) are one of the most widely used ingredients to stabilize food emulsions. They are partial hydrolysis products of starch consisting of α, 1–4 linked D-glucose chains of variable length. Some authors have reported the ability of MDX to protect oil-in-water emulsions against freezing destabilization (Ghosh et al., 2006; O'Regan and Mulvihill, 2010). However, there are no published works concerning about the effect of MDX on stability of multilayer linseed oil-in-water emulsions. Mun et al., 2008 reported the impact of MDX concentration on freeze-stability of corn oil-in-water multilayer emulsions, through particle size, ζ-potential and optical microscopy measurements. Nevertheless, they used relatively low oil concentration in their systems (2 wt% oil). Hence, in the present study, we propose to prepare emulsions with higher oil concentration (10 wt% oil) so as to make them more realistic to resemble food product matrices composition. However, this increase in the oil-phase volume fraction of emulsions could potentially enhance droplet–droplet interactions, thus altering their stability. In this context, the objective of this work was to study the influence of MDX concentration on the colloidal stability of linseed oil-in-water multilayer emulsions before and after freezing at different storage temperatures. In particular, we not only performed particle size, ζ-potential and optical microscopy measurements but also monitored emulsions backscattering destabilization profiles over time. This latter would help us understand when and why does phase separation occur in unstable systems.

2. Materials and methods

2.1. Materials

Milk whey protein isolate (WPI) was provided by Davisco Food International, Inc. (Minnesota, USA) and its composition (% w/w) was: 96.18% protein (N × 6.38) (dry basis), fat 0.20%, ash 1.90%, 5.57% moisture, 1.72% others. Low density sodium alginate (SA) was provided by Cargill (Buenos Aires, Argentina) (MW 135 kDa). As stated by the manufacturer the composition of this alginate was: carbohydrate 63%, moisture 14%, ash 23% (Na^+ 9300 mg/100 g and K^+ 800 mg/100 g). Maltodextrin obtained by enzyme hydrolysis of native corn starch (DE 15) was kindly donated by Productos de Maíz SA (Buenos Aires, Argentina). Linseed oil was obtained from Sigma Aldrich (St. Louis, MO) and it was used without further purification (density: 0.93 g/mL, refractive index: 1.48). All reagents were analytical grade.

2.2. Emulsion preparation

Mixed dispersions of 2 wt% WPI and 0–40 wt% MDX were prepared using Milli-Q ultrapure water and stirred for 2 h. Sodium alginate (SA) was dispersed in Milli-Q ultrapure water and stirred at 70 °C for 35 min to promote solubilization. The pH value of all dispersions was adjusted to 7.0 with HCl and NaOH (0.1 mol l^{-1}) and then dispersions were stored at 4 °C overnight. Primary emulsions were made by blending 20 wt% oil phase with 80 wt% aqueous WPI–MDX solutions using a high-speed blender (Waring Blender, Connecticut, USA) during 2 min at the highest velocity, followed by a sonication step (75% AMP, 150 s) performed by a 20 kHz ultrasonic probe with a 13 mm diameter tip (Sonics & Materials, Connecticut, USA). These emulsions were then diluted by adding sodium alginate (SA) dispersions and adjusting pH to 5 with HCl 2 N to form secondary emulsions, with the following final composition: 10 wt% oil, 1 wt% WPI 0.25 wt% SA and 0–20 wt% MDX. It should be highlighted that both WPI and SA concentrations as well as final pH value of secondary multilayer emulsions were identified in previous work as the optimum conditions to produce stable systems (Fioramonti et al., 2015). To assess the influence of freezing temperature on emulsion stability, they were stored for 7 days at −18 °C and 80 °C, respectively. After that period, they were incubated for 2 h in a water bath at 20 °C. Both fresh and thawed emulsions were analyzed just after being prepared.

2.3. Droplet size determination

Droplet size of emulsions was measured by static light scattering using a laser diffraction Mastersizer 2000 device with a Hydro 2000MU as a dispersion unit (Malvern Instruments, Worcestershire, Inglaterra). This is an optical technique that measures the intensity of the scattered light as a function of the scattering angle. The pump speed was settled between 900 and 1500 rpm. The refractive index of both the dispersed (1.48) and the continuous (1.33) phases was used. Droplet size is reported as the volume-mean diameter (D_{43}) and the equivalent volume-surface mean diameter (D_{32}):

$$D_{43} = \frac{\sum n_i d_i^4}{\sum n_i d_i^3} \quad (1)$$

$$D_{32} = \frac{\sum n_i d_i^3}{\sum n_i d_i^2} \quad (2)$$

where n_i is the number of droplets of diameter d_i (Lizarraga et al., 2008; Arzeni et al., 2012). Specific surface area (SSA) and polydispersity parameters obtained by the software are also reported. Polydispersity (or span) is related to the distribution width of droplet sizes as follows:

$$\text{Span} = \frac{(D_{0.9} - D_{0.1})}{D_{0.5}} \quad (3)$$

where 90%, 10% and 50% of the oil volume in the emulsions is contained in droplets with diameters below or equal to $D_{0.9}$, $D_{0.1}$ and $D_{0.5}$ respectively. The SSA was calculated using D_{32}, according to

$$\text{SSA} = \frac{6\phi}{D_{32}} \quad (4)$$

where ϕ represents the oil volume fraction of the emulsion (Gharibzahedi et al., 2013). Droplet sizes are reported as the average of ten readings made on each sample.

2.4. ζ-potential measurements

ζ-potential of emulsion droplets was determined by dynamic laser light scattering using a Zetasizer Nano-ZS instrument (Malvern Instruments, Worcestershire, England) as described in Fioramonti et al., 2015. Emulsions were diluted 1/1000 using double distilled water at pH 5, and were then injected into the measurement chamber. The ζ-potential was determined by measuring the direction and velocity of droplet movement in a well-defined electric field. These measurements are reported as the average and standard deviation of five determinations per sample.

2.5. Emulsion stability

Destabilization of emulsions was evaluated using a vertical scan analyzer Turbiscan TMA 2000 (Formulaction, Toulouse, France). The sample was placed in a cylindrical glass cell, and scanned from the bottom to the top with a laser light source ($\lambda = 850$ nm), as described in Fioramonti et al., 2015. Profiles recorded for each sample were then analyzed using the proper software, from which we obtained the creaming index, expressed as

$$\text{Creaming index } (\%) = \frac{H_S}{H_T} \cdot 100 \quad (5)$$

where H_S is the height of the serum layer, and H_T is the height of the total emulsion, as a parameter of global destabilization after 7 days of storage at room temperature. H_S was obtained from Turbiscan transmittance profiles, by measuring the thickness of the last peak (7 days) at 50% of the height (bottom zone). If there was no transmittance peak at 7 days of analysis, we considered $H_S = 0$. H_T was also obtained by Turbiscan profiles by measuring the height of the emulsion at initial time ($t = 0$) (Fioramonti et al., 2015).

2.6. Optical microscopy

Emulsions were properly stirred before analysis to ensure sample homogeneity. A drop of fresh emulsion was then placed between a microscope slide and a cover-slip and observed on a conventional optical microscope at a magnification of 40× (Leica Microsystems, Wetzlar, Germany).

2.7. Statistical analysis

All assays were measured at least in duplicate. Averages and standard deviations were calculated from these measurements. Differences between means were determined with LSD test at $p < 0.05$ significance level (Statgraphics Centurion XV).

3. Results and discussion

3.1. Effect of MDX concentration on droplet size distribution and droplet charge of emulsions

Droplet size distributions of emulsions at different MDX concentrations were determined by static light scattering (SLS). Malvern laser diffraction method generated a volume distribution for the analyzed light energy data, which was then converted to a number distribution using the proper software (Fig. 1A and B). The volume-mean diameter (D_{43}) and the volume-surface mean diameter (D_{32}), both derived from droplet size distributions, were used to characterize emulsions (Table 1). D_{43} is useful for the detection of large droplets whereas D_{32} is very sensitive to the presence of small droplets, as they have greater specific surface area (SSA) (Jafari et al., 2013). Polydispersity and SSA, are also listed in Table 1.

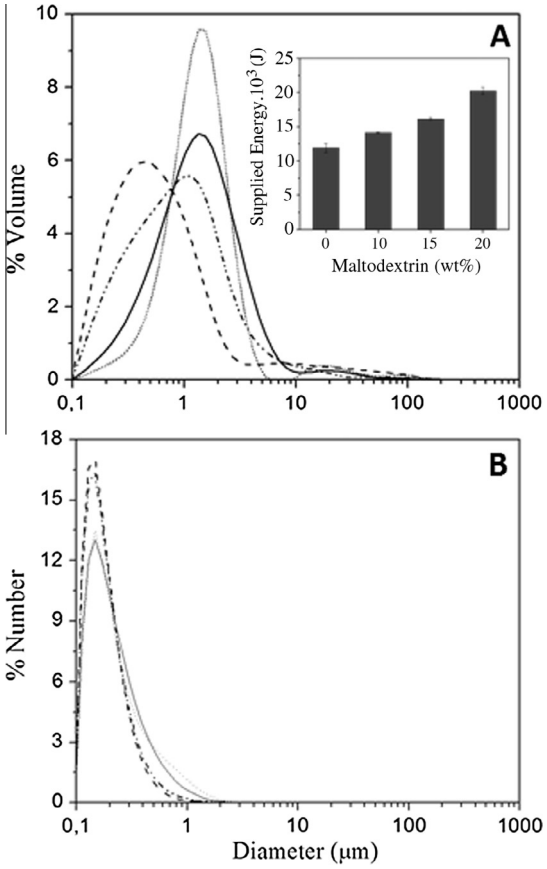

Fig. 1. Effect of MDX concentration (—0%, ···10%, —··15%, – – –20%) on volume (A) and number (B) droplet size distributions of 10 wt% oil 1 wt% WPI 0.25 wt% SA pH 5 emulsions. Inset (A): influence of MDX concentration on the total energy supplied to the systems by the ultrasonic probe.

Table 1
Volume-mean diameter D_{43}, volume-surface mean diameter D_{32}, polydispersity index (span) and specific surface area (SSA) of 10 wt% oil 1 wt% WPI 0.25% SA pH 5 emulsions, prepared at different MDX concentrations.

MDX (wt%)	D_{43} (μm)	Span	D_{32} (μm)	SSA (m^2/g)
0	2.41 ± 0.07^{a}	2.56 ± 0.06^{c}	0.88 ± 0.01^{f}	7.40 ± 0.06^{j}
10	2.78 ± 0.07^{b}	1.67 ± 0.07^{d}	1.04 ± 0.07^{g}	6.28 ± 0.42^{k}
15	1.96 ± 0.86^{a}	3.30 ± 0.20^{e}	0.52 ± 0.05^{h}	11.60 ± 0.99^{l}
20	$2.68 \pm 0.39^{a,b}$	4.73 ± 1.94^{e}	0.42 ± 0.02^{i}	15.65 ± 0.64^{m}

Data represent means ± standard deviations. Different letters indicate significant statistical differences ($p < 0.05$).

Emulsions containing 0 and 10 wt% MDX exhibited one predominant peak around 1 μm (Fig. 1A). The same trend was observed for 15 and 20 wt% MDX emulsions, where a left shift of the larger peak toward smaller sizes was detected, with a maximum around 1.02 μm and 0.45 μm, respectively. D_{43} showed no clear tendency when comparing emulsions with increasing MDX concentrations (Table 1). As this parameter represents an average of all droplet sizes for a particular system, it cannot adequately describe each population, especially when the system is not monodispersed. Emulsions prepared with 20 wt% MDX were the most polydisperse, as reflected by their span value (Table 1). Besides, it was observed that addition of MDX beyond 15 wt% produced a gradual increase of the SSA exhibited by emulsion droplets (Table 1). These results could be explained considering that MDX addition before homogenization could have modified the viscosity

ratio of dispersed to continuous phase. As the ultrasonic processor used to prepare primary emulsions was designed to deliver constant amplitude, the greater the resistance to the movement of the probe due to higher viscosity, the greater the amount of power delivered to the probe. This latter would supply a larger amount of energy to emulsions containing higher MDX concentrations (Fig. 1A inset). Since the total energy delivered to the systems is proportional to the interfacial area created (McClements, 1999), smaller droplet sizes, as reflected by D_{32} (Table 1), and higher SSA (Table 1) would be produced at higher MDX concentrations (15 wt% and 20 wt%). Klinkesorn et al., 2004, have found that addition of 10 wt% MDX (DE 15) to Tween 80-stabilized corn oil-in-water emulsions was not enough to appreciably increase the relative viscosity of the systems. Taking this into account, we suggest this could be the reason why 0 and 10 wt% emulsions presented similar droplet sizes (Fig. 1A, Table 1).

When converting volume size distribution (Fig. 1A) to a number-based one (Fig. 1B), it was found that the dominant population of droplets observed in Fig. 1B was the one corresponding to smaller sizes (<1 μm), with a maximum around 0.15 μm for all emulsions. Number size distributions overemphasize smaller sized droplets when compared to volume size distributions. This is because when calculating number-weighted diameters, small particles become more important, whereas for volume-weighted diameters, large particles are more relevant since they are related to d^3. Fig. 1B also revealed a greater number of smaller size droplets for emulsions containing 15 and 20 wt% MDX, which was consistent with the higher SSA created in these systems, as previously stated (Table 1). It bears noting that, although converting a volume result from laser diffraction to a number basis can lead to undefined errors, yet it could be useful to compare the relative importance of each droplet size population into the global distribution.

Zeta potential measurements were performed to evaluate the effect of MDX on electrostatic deposition of SA molecules onto the protein interfacial film surrounding the droplets (Fig. 2). In the absence of MDX, the ζ-potential of droplets in secondary emulsions (−54 mV) was more negative than that observed in primary emulsions (−11 mV), thus suggesting the adsorption of SA to the surface of WPI-coated droplets (Fioramonti et al., 2015). Considering that pH 5 is near WPI isoelectric point (4.7–5.2), it was expected for primary emulsions to have a relatively low magnitude of ζ-potential, as the protein net charge would be approaching to zero. However, as in these conditions local positively charged regions (or "patches") might be exposed on the protein surface, attractive interactions with negatively charged SA molecules

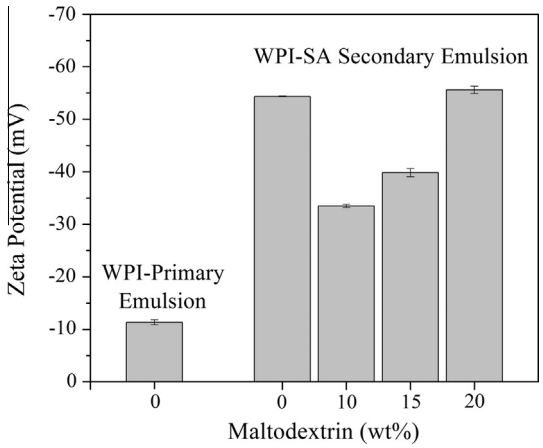

Fig. 2. Effect of MDX concentration on zeta potential of 10 wt% oil 1 wt% WPI pH 5 emulsions containing 0 wt% SA (primary emulsion) and 0.25 wt% SA (secondary emulsions).

present in secondary emulsions would be promoted, thereby forming a self-assembled interfacial bilayer (Fioramonti et al., 2015). When adding 10 wt% MDX to emulsions, the droplets ζ-potential changed from −54 mV to −33.5 mV, which would probably be indicating that less SA molecules might have been adsorbed onto the protein interface (Pongsawatmanit et al., 2006). However, it is interesting to note that at higher MDX concentrations the ζ-potential of droplets became more negative again, thus suggesting a greater number of SA molecules might have been adsorbed at the protein interface surrounding the droplets. Besides, it is noteworthy that systems containing 20 wt% MDX showed an ζ-potential value (−55 mV) close to that observed in emulsions without MDX. Although at first glance this may seem contradictory, a possible explanation for this phenomenon could be related to thermodynamic incompatibility between SA and MDX molecules in the continuous phase, when the bulk biopolymer concentration exceeds a critical level (Tolstoguzov, 2006). On the one hand, SA is a high MW (135,000 g/mol) linear binary copolymer composed of α-1,4 linked D-mannuronic and L-guluronic acid residues, arranged as homopolymeric blocks of consecutive monomers or altering M and G-residues along the chain. At pH 5, SA negatively charged carboxyl groups might exert electrostatic repulsion between them. Hence, it is expected that the macromolecule adopts a rigid rod-like extended conformation of maximum excluded volume in the aqueous phase so as to minimize repulsive electrostatic interactions. On the other hand, MDX is a neutral macromolecule of lower MW (DE 15, MW 1200 g/mol), so it would present a smaller effective volume in solution than SA molecules. Zhong et al., 2010 estimated a radius of gyration (R_g) for SA equal to 370 nm, whereas this parameter was expected to be near 1.7 nm for MDX (Klinkesorn et al., 2004). In this context, it could be possible that both polysaccharides remain cosoluble in the aqueous phase of 10 wt% MDX emulsions. Nevertheless, the presence of MDX molecules could have slightly increased the viscosity of the continuous phase of emulsions. This latter might have reduced the ability of SA molecules to flow, thereby preventing them from reaching the droplets' surface and decreasing their adsorption onto the protein interface to form an outer coating. In contrast, when adding higher MDX concentrations (15 and 20 wt%) to emulsions, thermodynamic incompatibility between biopolymers could have arised, mainly because of excluded volume effects and their competition for space in the aqueous phase (Perez et al., 2010). As a result of mutual exclusion of each polysaccharide from a volume occupied by macromolecules of the other, diffusion of negatively charged SA molecules toward positively charged protein interface could have been promoted through a segregative mechanism (Perez et al., 2009), thus increasing the magnitude of droplets ζ-potential (|ζ|) and making it more negative.

Besides, as previously discussed, emulsions containing 15 and 20 wt% MDX showed a greater number of droplets of smaller sizes (Fig. 1A and B) exposing a higher SSA (Table 1) than that observed for 10 wt% MDX emulsions. Consequently, SA molecules could have had a greater probability of encountering the droplets' surface and, thereby, more chances to electrostatically bind to the protein assembled at the oil–water interface.

In addition, it bears noting that all secondary emulsions presented ζ-potential values less than −30 mV, thus suggesting that electrostatic repulsion between the droplets would be sufficient to overcome attractive droplet–droplet interactions and stabilize emulsions (Guzey and McClements, 2004).

3.2. Effect of MDX concentration and freezing temperature on emulsion stability

The purpose of these experiments was to evaluate the influence of MDX on the stability of emulsions kept at different storage

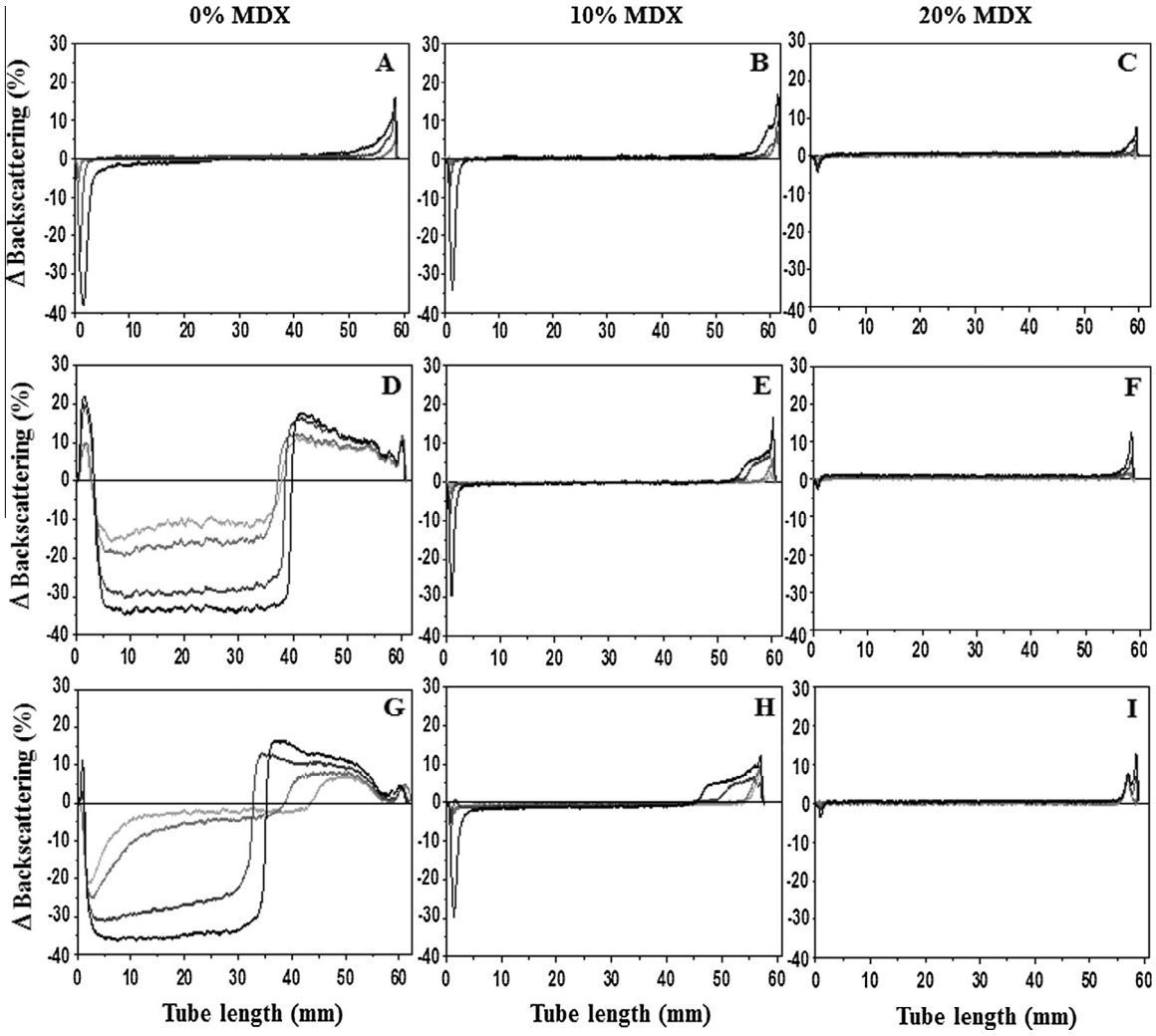

Fig. 3. Effect of MDX concentration (0 wt%: A, D, G; 10 wt%: B, E, H; 20 wt%: C, F, I) and freezing temperature (non-frozen: A, B, C; −18 °C: D, E, F; −80 °C: G, H, I) on the Δ Backscattering profiles of 10 wt% oil 1 wt% WPI 0.25 wt% SA pH 5 emulsions over time. Each curve corresponds to a single time measurement: 1 h (light gray), 2 h (gray), 24 h (dark gray), 7 days (black). (For interpretation of the references to color in this figure legend, the reader is referred to the web version of this article.)

temperatures (−18 and −80 °C) during freeze–thaw processing. As our systems were opaque and no light reached the transmission detector of Turbiscan, we analyzed their backscattering (BS) profiles as a function of the sample height, as shown in Fig. 3. These profiles constitute the macroscopic fingerprint of the emulsion sample at a given time (Mengual et al., 1999) and enabled us to examine the migration phenomena of lipid droplets. The curves are presented in a reference mode, where the first curve ($t = 0$) had been substracted from the subsequent ones ($\Delta BS = BS_t - BS_{t=0}$) in order to see the variations related to the initial state. The intensity of the backscattered light is related to the number of droplets located at a specific height of the emulsion. In our case, a reduction of Δ%BS represents a decrease in the number of droplets, whereas an increment of Δ%BS describes the opposite behavior. Fig. 4A shows the destabilization profile of an emulsion containing no MDX, before freeze–thaw cycling.

This represents a typical profile obtained by Turbiscan when creaming is the main mechanism of emulsion destabilization. It was observed that there was (i) a decrease in BS_t at the bottom of the sample related to a decrease of the concentration of the droplets in this part (clarification), and (ii) a concomitant increase of BS_t at the top of the sample due to an increase of the concentration of the dispersed phase and the formation of a cream layer. Creaming is a common phenomenon of instability for emulsions that is related to the upward movement of the droplets. The creaming velocity of an individual droplet is directly proportional to the square of its radius and to the density difference between the dispersed and the continuous phases, and inversely proportional to the viscosity of the continuous phase, as described by the Stokes law (McClements, 1999). When adding 10 wt% MDX (Fig. 3B), stability of emulsions seemed to be improved, as the peaks observed at the bottom of the tube (clarification zone) were clearly smaller than their 0 wt% MDX counterparts. The main differences were observed within the first two hours of measurement and after 24 h storage. This increased stability showed by 10 wt% MDX emulsions might be related to the narrower droplets size distribution obtained for these systems (Fig. 1A). As there would be less droplets of bigger sizes, their upward movement would be retarded (McClements, 1999). As shown by Fig. 3C, the most stable systems were obtained at the highest MDX concentration. It this case, not only did the presence of droplets of smaller sizes (Fig. 1A and B, Table 1) promote a greater stability, but also the higher MDX concentration (Klinkesorn et al., 2004). In fact, the increment of MDX concentration might have increased the density contrast between emulsion phases, which would accelerate creaming. However, this phenomenon could have been balanced by the increase of viscosity of the continuous phase, thus lowering creaming destabilization and enhancing emulsion stability. It should be

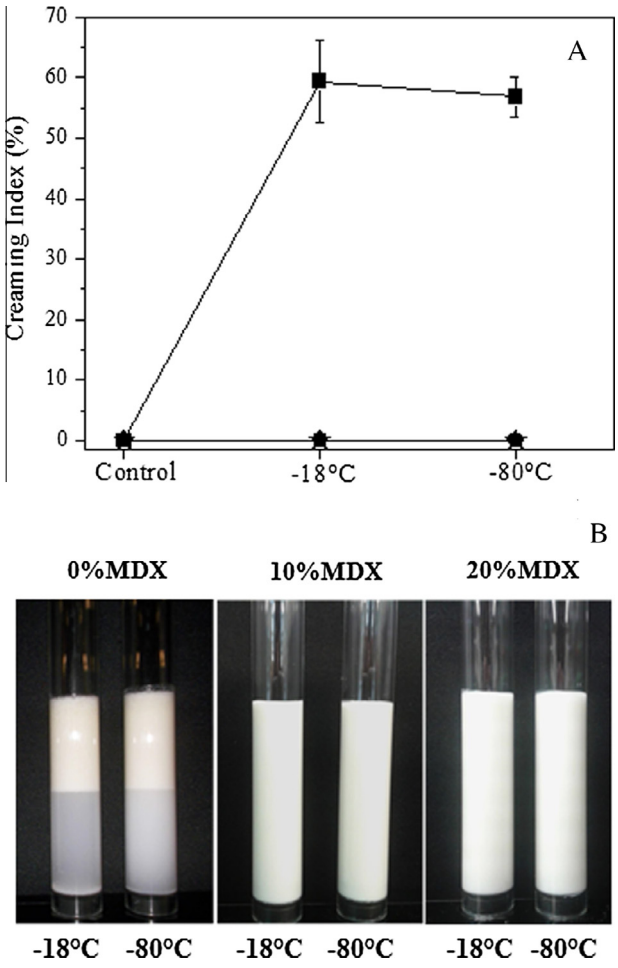

Fig. 4. Effect of freezing temperature and MDX concentration (■ 0 wt%, ● 10 wt%, ★ 20 wt%) on the creaming index of 10 wt% oil 1 wt% WPI 0.25 wt% SA pH 5 emulsions, after 1 week kept at ambient temperature. (B) Visual appearance of 10% oil 1%WPI 0.25%SA pH 5 thawed emulsions.

also highlighted that none of these emulsions exhibited macroscopic phase separation after seven days of analysis (visual appearance not shown). Indeed, as 15 wt% MDX systems presented a similar behavior to that observed for 20 wt% MDX emulsions, we did not include their profiles in Fig. 4.

The influence of freeze–thaw processing and MDX concentration on the stability of secondary emulsions was also studied. In the absence of MDX, rapid creaming was observed for emulsions stored at −18 °C and −80 °C (Fig. 3D and G). Emulsions kept at −18 °C exhibited almost immediate phase separation when thawed, as observed in Fig. 3D within the first hour of analysis. These systems also seemed to have sediment at the bottom of the sample cell, as reflected by the positive values of ΔBS between 0 and 4 mm tube length. On the other hand, in Fig. 3G it can be seen that emulsions stored at −80 °C presented a slower rate of destabilization within the first 2 h of analysis and less sediment formation at the bottom of the tube than their −18 °C counterparts. Nevertheless, they also showed phase separation at 24 h storage (Figs. 3G and 4B).

The low stability of these emulsions, in the absence of MDX, can be related to the crystallization of both the dispersed and the continuous phases. Ghosh and Coupland, 2008 suggested that freezing conditions might cause the rupture of interfacial membranes surrounding the droplets, promoting oil-to-oil contact. When water crystals are formed in the aqueous phase, emulsion droplets might become excluded from the space taken up by the ice, being forced into close proximity in the restricted phase volume remaining. Besides, ice crystals formed during freezing may penetrate into oil droplets and disrupt their interfacial membranes, thus making them more prone to coalesce once they are thawed (Gu et al., 2007).

The formation of an ice crystal is a two-step process that involves (i) a first nucleation stage, which occurs slowly and comprises the correct orientation of initial water molecules to give rise to a "nucleus" structure, and (ii) a second stage, where ice crystals rapidly grow from former nuclei (Vanapalli et al., 2002; Ghosh and Rousseau, 2009). Slower cooling rates, as the ones at −18 °C, would lead to the formation of larger ice crystals as there would be enough time to promote nucleation and subsequent growth of the crystals. This would lead to a greater extent of interfacial membranes disruption, and subsequent droplet coalescence. Besides, physical separation of ice during freezing implies a gradual concentration of solutes in the remaining aqueous phase (cryoconcentration) and a concomitant decrease of unfrozen water molecules (Martínez Navarrete et al., 1998). This latter would alter the conformation of self-assembled biopolymers at the oil–water interface, since there may be insufficient water to fully hydrate them, thereby enhancing the tendency of protein–polysaccharide complexes to desorb from the droplet surface and precipitate as a sediment once emulsion is thawed (Fig. 3D).

It is also interesting to highlight that in many food matrices, water freezing occurs at a fairly wide range of temperatures, between 0 °C and −40 °C, depending on the composition. Therefore, usual storage at −18 °C might not ensure (in most cases) the glassy state of the cryoconcentrated aqueous phase, which guarantees water immobilization and is only reached at temperatures below its glass transition temperature (T_g). The further the storage temperature is from the T_g, the more susceptible is the system to undergo ice recrystallization processes and progressive growth of crystals, as some water molecules could still flow in these conditions (Martínez Navarrete et al., 1998). So, this phenomenon would probably enhance formation of ice crystals of greater sizes during storage at −18 °C.

In contrast, if emulsion cooling rate is fast, like at −80 °C, ice crystals formation might be restricted by kinetic issues, as there would not be sufficient time to allow nucleation and crystal growth processes. As a result, smaller size ice crystals might be formed, thereby reducing both dehydration of biopolymers at the interfacial membrane (Fig. 3G) and droplet coalescence resulting from interfacial film disruption. Besides, at this storage temperature, it is likely that emulsion systems could be in their glassy state (below its T_g). If this were the case, the movement of water molecules would be restricted, thus inhibiting recrystallization processes (Martínez Navarrete et al., 1998).

Interestingly, frozen-thawed emulsions containing MDX, at each concentration, showed almost no relevant differences in their destabilization profiles when comparing both storage temperatures, with their respective non-frozen systems (Fig. 3E, F, H and I). The results obtained in our study about the influence of MDX on emulsion freeze–thaw stability are similar to those reported by Mun et al., 2008, and make evident the cryoprotective effect that MDX might have on emulsions during freezing. The presence of MDX (10 and 20 wt%) on the continuous phase of our emulsions could have inhibited ice crystals formation by several mechanisms. First, it is well-known that polysaccharides such as MDX have the ability to bind water molecules (Radosta and Schierbaum, 1990), thus making them unavailable for ice crystal formation. Secondly, the increment of MDX concentration, with a concomitant increase of the continuous phase viscosity, may also delay crystallization of water to form ice as it would slow down the diffusion rate of water molecules and, consequently, ice crystal formation. Taking this into account, increasing MDX concentration in the continuous phase of

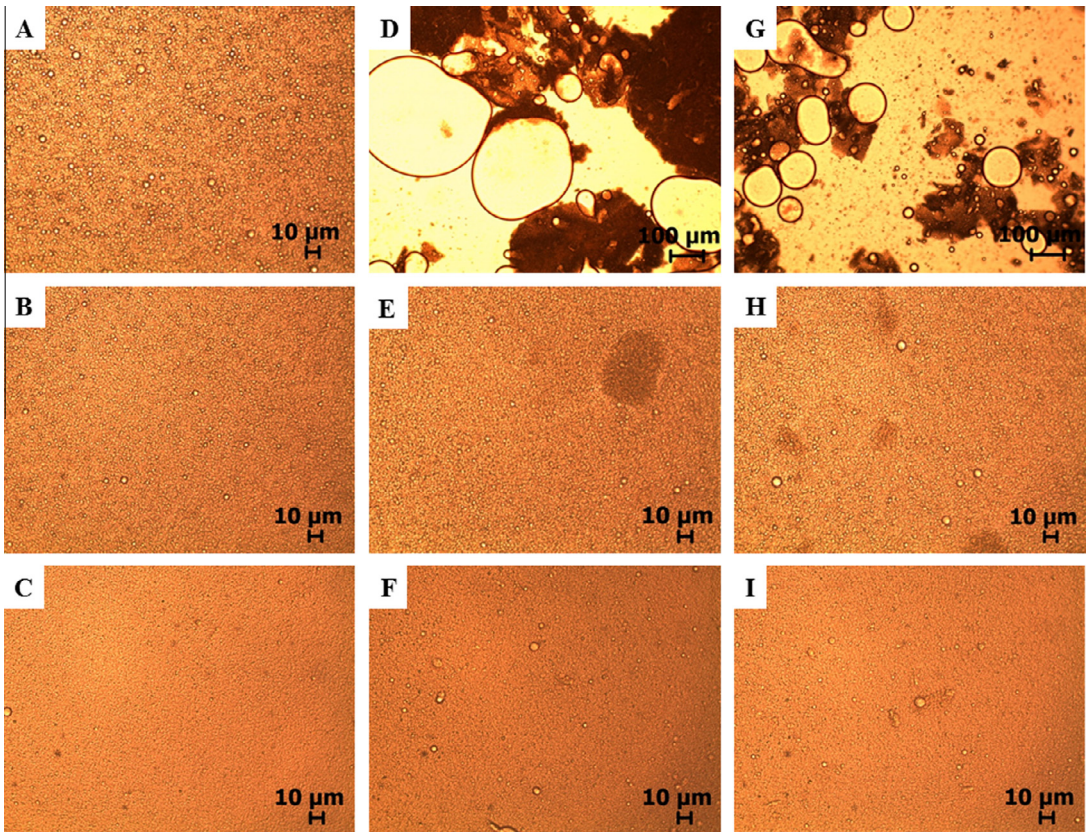

Fig. 5. Influence of MDX concentration and freezing temperature on the microstructure of 10 wt% oil 1 wt% WPI 0.25 wt% SA pH 5.

multilayer linseed oil-in-water emulsions would considerably reduce the amount of ice formed during freezing, and hence, the pressure exerted on the concentrated emulsion, thus reducing droplet–droplet interactions and coalescence. Besides, there would be a greater amount of unfrozen water molecules available to hydrate WPI and SA placed at the interface.

It should also be remembered that addition of high molecular weight solutes in the aqueous phase of emulsions, such as MDX, could greatly increase their T_g values. So, MDX could have also improved linseed oil multilayer emulsions stability by raising their T_g, thus ensuring the system glassy state at higher storage temperatures. As a result, ice recrystallization processes could be inhibited without requiring such low temperatures such as −80 °C, as it is likely that emulsions containing MDX would have reached their glassy state at −18 °C. Nevertheless, further work is needed to establish the influence of MDX concentration on the T_g value of emulsions.

Fig. 4A shows the effect of freezing temperature and MDX concentration on the creaming index of emulsions after 7 days of analysis. It can be seen that only frozen emulsions without MDX presented high creaming indexes and exhibited a macroscopic phase separation (Fig. 4B), whereas both unfrozen emulsions (control) and those freeze–thawed containing MDX were stable to creaming after one week storage.

Finally, in Fig. 5 the micrographs corresponding to the different studied systems are presented. From qualitative observation of unfrozen emulsions (Fig. 5A, B and C), one can verify the smaller droplet sizes presented by those containing 20 wt% MDX. In contrast, extensive droplet coalescence can be observed in frozen emulsions containing no MDX (Fig. 5D and G). Those storaged at −80 °C exhibited oil droplets of smaller sizes than the ones kept at −18 °C, this being consistent with the results previously discussed. Besides, it is easy to identify some dark patches exhibited in these latter systems (Fig. 5D and G), which could presumably correspond to those dehydrated protein–polysaccharide complexes that had precipitated as a sediment once emulsions were thawed (Fig. 3D, G and B).

On the other hand, frozen emulsions containing MDX were stable after thawed, presenting a slight variation of some droplet sizes (Fig. 5E, F, H and I). These results are consistent with those discussed above, and demonstrate the cryoprotective effect exerted by MDX on the studied emulsions.

4. Conclusions

Addition of maltodextrin to linseed oil-in-water multilayer emulsions greatly improved their stability. Higher MDX concentrations in emulsions that were not subjected to freeze–thaw processes produced smaller droplet sizes, thereby reducing creaming mechanisms and improving emulsion stability. When subject to freeze–thawing, emulsions without MDX were highly unstable and destabilized faster at −18 °C than at −80 °C, which was attributed to the formation of larger ice crystals at slower freezing rates that promoted extensive droplet coalescence. After 1 week storage, both systems presented macroscopic phase separation. Conversely, the presence of MDX exerted a cryoprotectant effect during freeze–thaw processes at both temperatures, as these emulsions did not show phase separation after thawing during one week storage at ambient temperature. These could be related to MDX water-binding properties and the increment in the amount of unfrozen water in the aqueous phase, thereby reducing the amount of ice formed during freezing. As a result, there would be more available water molecules to fully hydrate biopolymers adsorbed at the oil–water interface and the spacing matrix formed by MDX between droplets could have prevented them from coming into

contact, thus reducing coalescence mechanisms. It is therefore necessary to maintain the integrity of the interfacial membrane to ensure the preservation of original emulsion attributes after thawing, and to avoid destabilizing processes such as droplet coalescence and oiling off. The results of this study have shown that 20 wt% MDX emulsions were the most stable systems both to creaming destabilization and to freeze–thaw processes. This may have important consequences for the development of food matrices with improved resistance to low temperature storage.

Acknowledgements

This research was supported by the following projects: CAI+D PI 2011 (50120110100171LI) and CATT 2011 (Proyecto Cambio de Escala), both from Universidad Nacional del Litoral (UNL, Argentina). Authors would like to thank María Julia Martínez for her advice and kind collaboration on droplet size and zeta-potential determinations. We also want to acknowledge for the financial support of Consejo Nacional de Investigaciones Científicas y Técnicas de la República Argentina (CONICET).

References

Arzeni, C., Pérez, O.E., Pilosof, A.M.R., 2012. Functionality of egg white proteins as affected by high intensity ultrasound. Food Hydrocolloids 29, 308–316.
Carneiro, H.C.F., Tonon, R.V., Grosso, C.R.F., Hubinger, M.D., 2013. Encapsulation efficiency and oxidative stability of flaxseed oil microencapsulated by spray drying using different combinations of wall materials. J. Food Eng. 115 (4), 443–451.
Fioramonti, S.A., Martínez, M.J., Pilosof, A.M.R., Rubiolo, A.C., Santiago, L.G., 2015. Multilayer emulsions as a strategy for linseed oil microencapsulation: effect of pH and alginate concentration. Food Hydrocolloids 43, 8–17.
Gharibzahedi, S.M.T., Razavi, S.H., Mousavi, S.M., 2013. Ultrasound-assisted formation of the canthaxanthin emulsions stabilized by arabic and xanthan gums. Carbohydr. Polym. 96, 21–30.
Ghosh, S., Coupland, J.N., 2008. Factors affecting the freeze–thaw stability of emulsions. Food Hydrocolloids 22, 105–111.
Ghosh, S., Rousseau, D., 2009. Freeze–thaw stability of water-in-oil emulsions. J. Colloid Interface Sci. 339, 91–102.
Ghosh, S., Cramp, G.L., Coupland, J.N., 2006. Effect of aqueous composition on the freeze–thaw stability of emulsions. Colloids Surf., A 272, 82–88.
Gu, Y.S., Decker, E.A., McClements, D.J., 2007. Application of multi-component biopolymer layers to improve the freeze–thaw stability of oil-in-water emulsions: β-lactoglobulin-ι-carrageenan–gelatin. J. Food Eng. 80, 1246–1254.
Guzey, D., McClements, D.J., 2004. Impact of electrostatic interactions on formation and stability of emulsions containing oil droplets coated by beta-lactoglobulin–pectin complexes. J. Agric. Food Chem. 55, 475–485.
Guzey, D., McClements, D.J., 2006. Formation, stability and properties of multilayer emulsions for application in the food industry. Adv. Colloid Interface Sci. 128, 227–248.
Innis, S., 2007. Dietary ω-3 fatty acids and brain development. J. Nutr. 137, 855–859.
Jafari, S.M., Beheshti, P., Assadpour, E., 2013. Emulsification properties of a novel hydrocolloid (Angum gum) for D-limonene droplets compared with Arabic gum. Int. J. Biol. Macromol. 61, 182–188.
Klinkesorn, U., Sophanodora, P., Chinachoti, P., McClements, D.J., 2004. Stability and rheology of corn oil-in-water emulsions containing maltodextrin. Food Res. Int. 37, 857–859.
Lizarraga, M.S., Pan, L.G., Añón, M.C., Santiago, L.G., 2008. Stability of concentrated emulsions measured by optical and rheological methods. Effect of processing conditions – I. Whey protein concentrate. Food Hydrocolloids 22, 868–878.
Martínez Navarrete, N., Andrés Grau, A.M., Chiralt Boix, A., Maupoey, P.F., 1998. Termodinámica y cinética de sistemas alimento entorno ed. Universidad Politécnica de Valencia, España.
McClements, D.J., 1999. Food Emulsions: Principles, Practice, and Techniques. CRC Press, Boca Ratón, Florida, USA.
McClements, D.J., Decker, E.A., Weiss, J., 2007. Emulsion-based delivery systems for lipophilic bioactive components. J. Food Sci. 72 (8), 109–124.
Mengual, O., Meunier, G., Cayré, I., Puech, K., Snabre, P., 1999. Turbiscan MA 2000: multiple light scattering measurement for concentrated emulsion and suspension instability analysis. Talanta 50 (2), 445–456.
Mun, S., Cho, Y., Decker, E.A., McClements, D.J., 2008. Utilization of polysaccharide coatings to improve freeze–thaw and freeze–dry stability of protein-coated lipid droplets. J. Food Eng. 86, 508–518.
O'Regan, J., Mulvihill, D., 2010. Heat stability and freeze–thaw stability of oil-in water emulsions stabilised by sodium caseinate–maltodextrin conjugates. Food Chem. 119, 182–190.
Palazolo, G.G., Sobral, P.A., Wagner, J.R., 2011. Freeze-thaw stability of oil-in-water emulsions prepared with native and thermally-denatured soybean isolates. Food Hydrocolloids 25, 398–409.
Perez, A.A., Carrara, C.R., Sánchez, C.C., Santiago, L.G., Rodríguez Patino, J.M., 2009. Interfacial dynamic properties of whey protein concentrate/polysaccharide mixtures at neutral pH. Food Hydrocolloids 23 (5), 1253–1262.
Perez, A.A., Sánchez, C.C., Patino, J.M.R., Rubiolo, A.C., Santiago, L.G., 2010. Milk whey proteins and xanthan gum interactions in solution and at the air–water interface: a rheokinetic study. Colloids Surf., B 81 (1), 50–57.
Pongsawatmanit, R., Harnsilawat, T., McClements, D.J., 2006. Influence of alginate, pH and ultrasound treatment on palm oil-in-water emulsions stabilized by β-lactoglobulin. Colloids Surf., A 287, 59–67.
Radosta, S., Schierbaum, F., 1990. Polymer–water interaction of maltodextrins. Starch – Stärke 4, 142–147.
Rodea-González, D.A., Cruz-Olivares, J., Román-Guerrero, A., Rodríguez-Huezo, M.E., Vernon-Carter, E.J., Pérez-Alonso, C., 2012. Spray-dried encapsulation of chia essential oil (*Salvia hispanica* L.) in whey protein concentrate-polysaccharide matrices. J. Food Eng. 111, 102–109.
Thanasukarn, P., Pongsawatmanit, R., McClements, D.J., 2006. Utilization of layer-by-layer interfacial deposition technique to improve freeze–thaw stability of oil-in-water emulsions. Food Res. Int. 39, 721–729.
Tolstoguzov, V., 2006. Food Polysaccharides and Their Applications, second ed. CRC/Taylor & Francis, Boca Raton, FL.
Vanapalli, S.A., Palanuwech, J., Coupland, J.N., 2002. Stability of emulsions to dispersed phase crystallization: effect of oil type, dispersed phase volume fraction, and cooling rate. Colloids Surf., A 204, 227–237.
Wu, N., Huang, X., Yang, X., Guo, J., Zheng, E., Yin, S., Zhu, J., Qi, J., He, X., Zhang, J., 2012. Stabilization of soybean oil body emulsions using ι-carrageenan: effects of salt, thermal treatment and freeze–thaw cycling. Food Hydrocolloids 28, 110–120.
Zhong, D., Huang, X., Yang, H., Cheng, R., 2010. New insights into viscosity abnormality of sodium alginate aqueous solution. Carbohydr. Polym. 81, 948–952.